

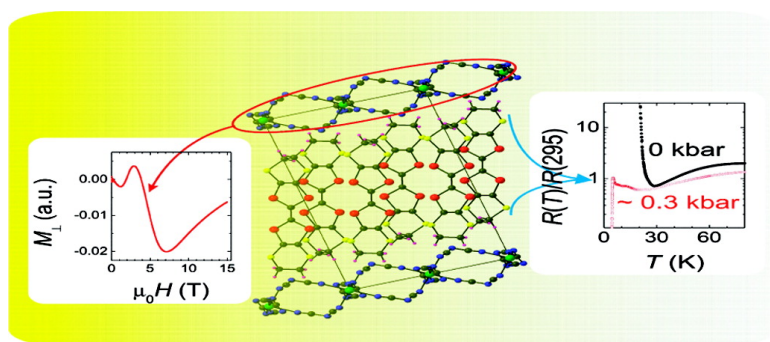
Communication

#-Donor BETS Based Bifunctional Superconductor with Polymeric Dicyanamidomanganate(II) Anion Layer: #- $(\text{BETS})\text{Mn}[\text{N}(\text{CN})]$

Nataliya D. Kushch, Eduard B. Yagubskii, Mark V. Kartsovnik, Lev I. Buravov,
 Alexander D. Dubrovskii, Anatolii N. Chekhlov, and Werner Biberacher

J. Am. Chem. Soc., **2008**, 130 (23), 7238-7240 • DOI: 10.1021/ja801841q • Publication Date (Web): 16 May 2008

Downloaded from <http://pubs.acs.org> on February 8, 2009



More About This Article

Additional resources and features associated with this article are available within the HTML version:

- Supporting Information
- Access to high resolution figures
- Links to articles and content related to this article
- Copyright permission to reproduce figures and/or text from this article

[View the Full Text HTML](#)

π -Donor BETS Based Bifunctional Superconductor with Polymeric Dicyanamidomanganate(II) Anion Layer: κ -(BETS)₂Mn[N(CN)₂]₃

Nataliya D. Kushch,^{*,†} Eduard B. Yagubskii,[†] Mark V. Kartsovnik,^{*,‡} Lev I. Buravov,[†]
Alexander D. Dubrovskii,[†] Anatolii N. Chekhlov,[†] and Werner Biberacher[‡]

*Institute of Problems of Chemical Physics, Russian Academy of Science, Chernogolovka, 142432 Russia, and
Walther-Meissner-Institut, Bayerische Akademie der Wissenschaften, Walther-Meissner-Strasse 8, Garching D-85748,
Germany*

Received March 12, 2008; E-mail: kushch@icp.ac.ru; mark.kartsovnik@wmi.badw-muenchen.de

A new trend in chemistry and physics of radical cation salts appeared and has been developed over the past decade, aiming at the design of hybrid multifunctional molecular materials combining conducting and magnetic properties in the same crystal lattice. In such materials, electrical conductivity is provided by an organic radical cation subsystem while magnetism is provided by an anionic subsystem, containing magnetic transition metal ions.

The combination of conductivity and magnetism in crystals of radical cation salts and their synergism give rise, in some cases, to unique materials and novel physical properties. For example, magnetic field induced superconductivity has recently been found in λ -(BETS)₂FeCl₄¹⁻³ and κ -(BETS)₂FeBr₄.^{3,4} Such materials are of high interest as possible objects for spintronics due to their gigantic magnetoresistance effect. By now, among radical cation salts, a number of metals and superconductors with localized magnetic moments,⁵⁻⁷ as well as molecular antiferromagnetic metals and superconductors^{3,8-10} and ferromagnetic metals^{11,12} have been prepared and intensely studied. Magnetic properties of these salts are provided by the presence of metal complex anions based on transition d-metals and possessing halide, CN, or oxalate ions as ligands. Recently, first radical cation salts of BEDT-TTF with magnetic dicyanamidometallate anions have been prepared: (BEDT-TTF)₂Mn[N(CN)₂]₃ and (BEDT-TTF)₂CuMn[N(CN)₂]₄.^{13,14}

This paper reports on the structure and properties of the radical cation salt based on π -donor BETS (BETS = bis(ethylenedithio)tetraselenafulvalene) with tri(dicyanamido)manganate(II) anion: (BETS)₂Mn[N(CN)₂]₃. By contrast to a semiconducting behavior of the BEDT-TTF salt with the same anion, the present compound is metallic down to low temperatures and becomes superconducting under a moderate pressure of ~ 0.3 kbar.

The main crystallographic data for (BETS)₂Mn[N(CN)₂]₃¹⁵ are: monoclinic structure, $a = 19.507(4)$ Å, $b = 8.4120(10)$ Å, $c = 12.104(2)$ Å, $\beta = 91.85(2)^\circ$, $V = 1985.1(6)$ Å³, space group $P2_1/c$, $z = 2$; $R_1 = 0.0392$, CCDC 679003. The crystal structure of the salt is characterized by the alternation of κ -type organic radical cation layers with layers composed of polymeric Mn[N(CN)₂]₃ anions along the a axis of the unit cell (Figure 1). Similarly to other κ -salts, the conducting layers in the κ -(BETS)₂Mn[N(CN)₂]₃ crystals are formed by the BETS dimers with +0.5 averaged charge per molecule. The dihedral angle between the neighboring dimers is 72.8° . Similar values of the dihedral angle ($77-80^\circ$) were also found in other κ -BETS salts.¹⁶ The BETS radical cations in the dimer are overlapped as «ring over bond» type.¹⁷ Such overlapping mode is realized in all superconductors with the κ -type conducting layers. One of terminal ethylene groups in the BETS

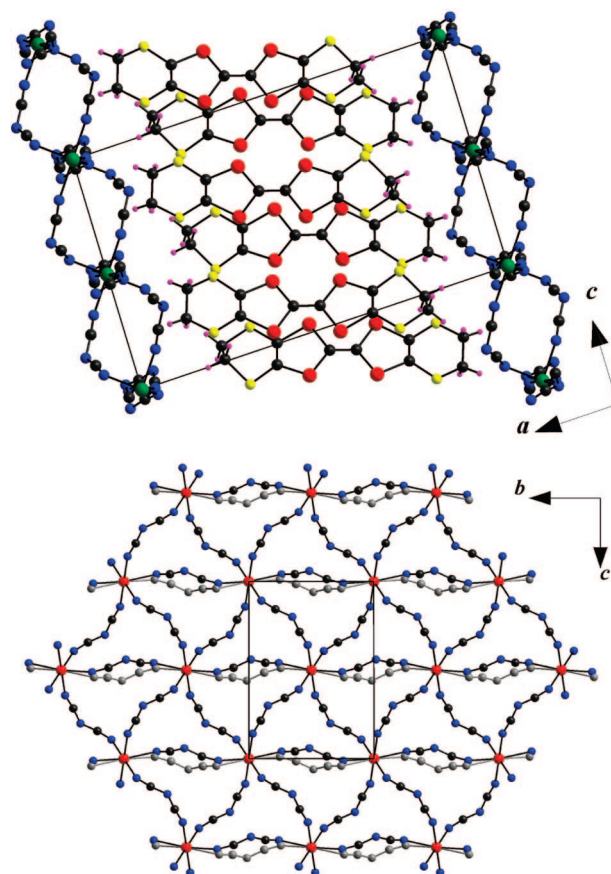


Figure 1. Crystal structure of κ -(BETS)₂Mn[N(CN)₂]₃ projected on the ac plane (top) and projection of the anion layer on the bc plane (bottom).

radical cation is disordered that gives rise to two possible conformers (eclipsed, e , and staggered, s , conformations). The $e:s$ conformers ratio is 0.20:0.80. A similar ratio was found in κ -salts of the (BEDT-TTF)₂Cu[N(CN)₂]Cl family.¹⁸ There are several short intermolecular contacts, S \cdots S (3.458–3.581 Å), Se \cdots S (3.445, 3.593 Å), and C–H \cdots S (2.847–2.999 Å), in the structure of the radical cation layer. Additionally to these contacts, each radical cation in the conducting layer is bound with the anion layer by hydrogen C–H \cdots N (2.549–2.725 Å) bonds and one S \cdots N contact which is 0.082 Å shorter than the sum of van der Waals radii of sulfur and nitrogen. The S \cdots N contact is formed only with the central nitrogen atom of the –NC–N–CN– ligand, while the hydrogen bonds are formed with all nitrogen atoms.

[†] Russian Academy of Science.

[‡] Walther-Meissner-Institut.

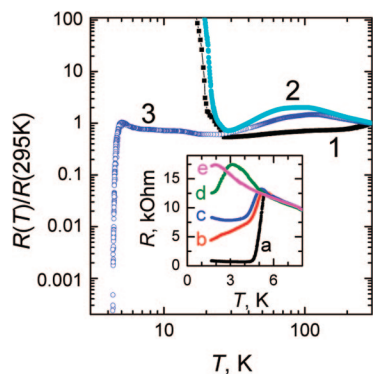


Figure 2. Temperature dependence of the resistance of κ -(BETS) $_2$ Mn[N(CN) $_2$] $_3$ measured parallel to conducting radical cation layers (curve 1) and perpendicular to them (curve 2) at ambient pressure, and the interlayer resistance under a pressure of ~ 0.3 kbar created by cooling in GKZh oil (curve 3). Inset: Superconducting transition in the interlayer resistance of another sample cooled in GKZh, at zero magnetic field (a) and at fields of 0.01 T (b), 0.03 T (c), 0.7 T (d), and 1.6 T (e), directed perpendicular to layers.

The polymeric Mn[N(CN) $_2$] $_3^-$ anion is formed by one independent Mn atom located in the inversion center and two independent $-N(CN)_2-$ ligands (Figure 1). Like in the BEDT-TTF salt of a similar composition, 13,14 each Mn atom has an octahedral environment and is linked with six neighboring metal atoms via $\mu_{1,5}$ -N(CN) $_2$ bridges. In contrast to the (BEDT-TTF) $_2$ Mn[N(CN) $_2$] $_3$ salt, 13 in which the anion is ordered, in the anion layer of the present κ -salt, one dicyanamide group located along the b axis of the unit cell is statistically disordered.

Room-temperature conductivity of the crystals along conducting layers and perpendicular to them was measured to be $5\text{--}30\text{ Ohm}^{-1}\text{ cm}^{-1}$ and $5 \times 10^{-4}\text{ Ohm}^{-1}\text{ cm}^{-1}$, respectively. The temperature dependences of the inplane and interplane resistances are shown in Figure 2. The inplane resistance decreases by approximately a factor of 2 by lowering temperature from 295 K down to $T_{\text{min}} \approx 28$ K and then rapidly grows (curve 1 in Figure 2). The interplane resistance (curve 2 in Figure 2) gradually increases at cooling from room temperature until ~ 100 K and decreases at further cooling to T_{min} . Such a behavior of interlayer resistance $R_{\perp}(T)$ is typical of many layered organic metals and is most likely caused by a breakdown of the interlayer transport coherence and strong electron–phonon interactions. 19 Below T_{min} , the interlayer resistance shows a dramatic increase, like in the case of the inplane measurements, indicating a metal–insulator (MI) transition. The transition temperature defined as that of the minimum in the logarithmic derivative $d(\ln R_{\perp})/dT$ 20 is $T_1 \approx 21$ K.

The observed transition is extremely sensitive to pressure. Curve 3 in Figure 2 shows the resistance $R_{\perp}(T)$ of a crystal placed inside a drop of silicon oil GKZh-136. Due to a difference in thermal contractions, a pressure of 0.2–0.4 kbar is generated by cooling to low temperatures. 21 As a result, the low-temperature increase of resistance is almost completely suppressed and the sample undergoes a superconducting transition at $T_c \approx 4.5$ K. This behavior has been reproduced on several samples. As an example, the inset in Figure 2 shows the low-temperature interlayer resistance of another crystal placed in GKZh oil, recorded in different magnetic fields. For this sample, the resistance does not reach zero below T_c , saturating at the level of 4% of the normal-state resistance. Nevertheless, the superconducting nature of the transition is ascertained by its high sensitivity to a magnetic field.

A qualitatively similar behavior has been observed on another organic conductor, λ -(BETS) $_2$ FeCl $_4$. In that compound, the MI

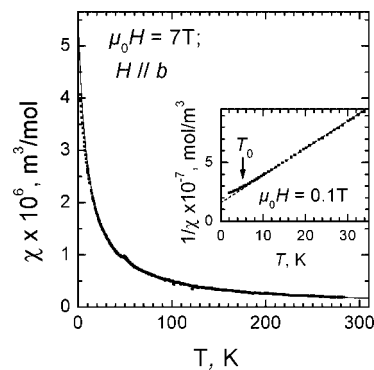


Figure 3. Temperature dependence of magnetic susceptibility in the field parallel to the b axis; the solid line is a fit to the Curie–Weiss law (see text). Inset: Inverse susceptibility $1/\chi(T)$ in a weak magnetic field, $\mu_0H = 0.1\text{ T} \ll k_B T/g\mu_{\text{eff}}$. The deviation from the linear dependence below T_0 indicates an onset of AFM ordering.

transition at 8.3 K is associated with an antiferromagnetic (AFM) ordering in the system of Fe^{3+} ions and a exchange interaction between 3d electrons of iron and conducting π electrons in cation layers. 2,22 The AFM insulating state can be suppressed by a magnetic field of 12 T; 22 moreover, in fields $17\text{ T} < \mu_0H < 42\text{ T}$ parallel to layers a superconducting state is observed. 1,2 Further, the π –d interaction is weakened under pressure: a pressure ≥ 3 kbar stabilizes the metallic state 23 with a superconducting transition at 2 K. 9 Noteworthy, in comparison to λ -(BETS) $_2$ FeCl $_4$, the MI transition in our compound is suppressed by a much lower pressure and the pressure-induced superconducting state shows a higher T_c . On the other hand, a magnetic field of 15 T shifts the MI transition temperature by no more than ~ 0.5 K. The relative weakness of the field effect in our compound in comparison to that in λ -(BETS) $_2$ FeCl $_4$ is not surprising, keeping in mind the 3 times higher temperature of the MI transition.

Given the presence of magnetic ions Mn^{2+} in κ -(BETS) $_2$ Mn[N(CN) $_2$] $_3$, one can also expect here interesting effects of an interaction between the magnetic and conducting subsystems. It should be noted, however, that the structures of the magnetic anion layers are considerably different in the present salt and in the salts of BETS with the FeX_4 (where $X = \text{Cl}, \text{Br}$) anions. In the latter compounds, anion layers are built of discrete paramagnetic units FeX_4^- , and the exchange interaction between them is established through π -electrons of cation layers. In κ -(BETS) $_2$ Mn[N(CN) $_2$] $_3$, the anion layers have a polymeric structure with paramagnetic ions Mn^{2+} connected via dicyanamide bridges. This should favor a direct exchange interaction within the anion layers, as it happens in the salt (BEDT-TTF) $_2$ Mn[N(CN) $_2$] $_3$. 14 On the other hand, an analysis of shortened contacts between anion and radical cation layers in the structure of the present salt suggests a possibility of π –d interactions via nitrogen 2p orbitals. With this in mind, we have performed a study of magnetic properties of this compound.

Figure 3 shows the temperature dependence of molar magnetic susceptibility χ of a single crystal with a mass of 95 μg obtained on a SQUID magnetometer. The magnetic field, $\mu_0H = 7\text{ T}$, is applied parallel to conducting layers, along the crystallographic short axis b . In the whole temperature range, except the lowest temperatures, susceptibility nicely follows the Curie–Weiss law for localized paramagnetic spins, $\chi = C_m/(T - \theta)$ (a small peak at ~ 50 K was not reproduced in successive measurements in the interval 35–60 K; it is, most likely, associated with oxygen remnant in the sample space). The Curie constant, $C_m = (5.2 \pm 0.2) \times 10^{-5}\text{ m}^3 \cdot \text{K/mol}$, yields an effective magnetic moment, $\mu_{\text{eff}} = (5.8$

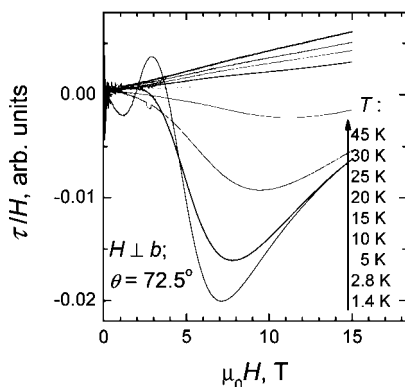


Figure 4. Magnetic torque, scaled to the field strength, as a function of the field aligned in the ac plane, at different temperatures; θ is the angle between the c axis and the magnetic field direction.

$\pm 0.1)\mu_B$ (μ_B being the Bohr magneton), indicating that magnetization is dominated by the high-spin, $S = 5/2$, state of Mn^{2+} ions. The negative Curie–Weiss temperature, $\theta = -9.7$ K, reveals AFM correlations between the paramagnetic spins. Note that it is close to the value found in the relative BEDT-TTF based salt.¹³ No significant changes in the susceptibility behavior occur in the temperature range corresponding to the MI transition; the inverse susceptibility, $1/\chi$, keeps the linear temperature dependence, as shown in the inset in Figure 3. However, at cooling below $T_0 \approx 5$ K, a considerable deviation from the Curie–Weiss behavior signaling an onset of AFM ordering is observed.

The AFM ordering is also clearly manifested in magnetic torque τ measured in a magnetic field inclined with respect to the principal axes of the susceptibility tensor. The results of torque measurements in the field directed in the crystallographic ac plane, at an angle of $\sim 73^\circ$ from the c axis, are presented in Figure 4. The ratio $\tau(H)/H$ plotted along the Y axis is proportional to the magnetization component perpendicular to the external field, M_\perp (taking into account that $M \ll H$). At cooling below T_0 , in fields below 4 T, an anomaly originating most likely from the spin-flop transition in the AFM state rapidly develops. In addition, the curves $\tau(H)/H$ exhibit a nonmonotonic shape in higher fields, with a minimum at 7–10 T. The corresponding deviations from a usual paramagnetic monotonic field dependence arise already at a temperature of ~ 20 K, that is, around the MI transition. One can, therefore, suggest a correlation between the phase transformation in the conduction system and the evolution of magnetic properties of insulating layers.

The origin of the anomalous high-field behavior of magnetic torque at temperatures $T \leq 20$ K is not clear at present. The absence of anomalies in the $\chi(T)$ curve taken on the SQUID magnetometer from the same sample (see inset in Figure 3) implies that a reorientation of spins takes place most likely in the plane perpendicular to the b axis. Further detailed studies in magnetic fields are necessary for clarifying the nature of the low-temperature magnetic state and its influence on the conduction system in κ -(BETS)₂Mn[N(CN)₂]₃.

In summary, crystals of κ -(BETS)₂Mn[N(CN)₂]₃ were synthesized and their structure was examined. The crystals show a

transition into a superconducting state with $T_c \approx 5$ K at $P = 0.3$ kbar. At ambient pressure, the compound exhibits a metal–insulator transition at $T_I \approx 21$ K and an AFM ordering at $T_0 \approx 5$ K. Although the temperatures T_I and T_0 are considerably different, distinct changes in the magnetic torque behavior starting near T_I suggest that π – d interactions play important role in the present system.

Acknowledgment. We thank Prof. A. Kobayashi for BETS used in the work, and the RFBR Projects No 07-02-91562 DFG (RUS 113/926/0-1), No. 07-03-91207 JSPS and No. 06-02-16471 for financial support.

Supporting Information Available: Synthesis of Mn[N(CN)₂]₂, cif file, and details of the study of structure, resistivity, and magnetic properties of the κ -(BETS)₂Mn[N(CN)₂]₃ crystals. This material is available free of charge via the Internet at <http://pubs.acs.org>.

References

- (1) Uji, S.; Shinagawa, H.; Terashima, T.; Yakabe, T.; Terai, Y.; Tokumoto, M.; Kobayashi, A.; Tanaka, A.; Kobayashi, H. *Nature* **2001**, *410*, 908.
- (2) Balicas, L.; Brooks, J. S.; Storr, K.; Uji, S.; Tokumoto, M.; Tanaka, H.; Kobayashi, H.; Kobayashi, A.; Barzykin, V.; Gorkov, L. P. *Phys. Rev. Lett.* **2001**, *87*, 067002.
- (3) Kobayashi, H.; Cui, H.; Kobayashi, A. *Chem. Rev.* **2004**, *104*, 5265.
- (4) Fujiwara, H.; Kobayashi, H.; Fujiwara, E.; Kobayashi, A. *J. Am. Chem. Soc.* **2002**, *124*, 6816.
- (5) Prokhorova, T. P.; Khasanov, S. S.; Zorina, L. V.; Buravov, L. I.; Tkacheva, V. A.; Baskakov, A. A.; Morgunov, R. B.; Gener, M.; Canadell, E.; Shibaeva, R. P.; Yagubskii, E. B. *Adv. Funct. Mater.* **2003**, *13*, 403.
- (6) Martin, L. L.; Turner, S. S.; Day, P.; Mabbs, F. E.; Meinel, E. J. L. *Chem. Commun.* **1997**, 1367.
- (7) Kurmoo, M.; Graham, A. W.; Day, P.; Coles, S. J.; Hursthouse, M. B.; Caulfield, J. M.; Singleton, J.; Ducas, L.; Guionneau, P. *J. Am. Chem. Soc.* **1995**, *117*, 12209.
- (8) Tanaka, H.; Adachi, T.; Ojima, E.; Fujiwara, H.; Kato, K.; Kobayashi, H. *J. Am. Chem. Soc.* **1999**, *121*, 11243.
- (9) Otsuka, T.; Cui, H. B.; Fujiwara, H.; Kobayashi, H.; Fujiwara, E.; Kobayashi, A. *J. Mater. Chem.* **2004**, *14*, 1682.
- (10) Choi, E. S.; Graf, D.; Brooks, J. S.; Yamada, J.; Akutsu, A.; Kikuchi, K.; Tokumoto, M. *Phys. Rev.* **2004**, *B 70*, 024517.
- (11) Coronado, E.; Galan-Mascaros, J. R.; Gomez-Garcia, C. J.; Laukhin, V. *Nature* **2000**, *408*, 447.
- (12) Alberola, A.; Coronado, E.; Galan-Mascaros, J. R.; Gimenez-Saiz, C.; Gomez-Garcia, C. J. *J. Am. Chem. Soc.* **2003**, *125*, 10774.
- (13) Schlüter, J.; Geiser, U.; Manson, L. J. *J. Phys. IV Fr.* **2004**, *114*, 475.
- (14) Kusch, N. D.; Kazakova, A. V.; Dubrovskii, A. D.; Shilov, G. V.; Buravov, L. I.; Morgunov, R. B.; Kurganova, E. V.; Tanimoto, Y.; Yagubskii, E. B. *J. Mater. Chem.* **2007**, *17*, 4407.
- (15) Crystals of κ -(BETS)₂Mn[N(CN)₂]₃ were prepared by electrocrystallization from 1,1,2-trichloroethane plus ethanol solution containing BETS and Mn[N(CN)₂]₂ salt.
- (16) (a) Narymbetov, B. Zh.; Kusch, N. D.; Zorina, L. V.; Khasanov, S. S.; Shibaeva, R. P.; Togonidze, T. G.; Kovalev, A. E.; Kartsovnik, M. V.; Buravov, L. I.; Yagubskii, E. B.; Canadell, E.; Kobayashi, A.; Kobayashi, H. *Eur. Phys. J.* **1998**, *B5*, 179. (b) Kobayashi, A.; Udagava, T.; Tomita, H.; Naito, T.; Kobayashi, H. *Chem. Lett.* **1993**, 2179.
- (17) Mori, T.; Mori, H.; Tanaka, S. *Bull. Chem. Soc. Jpn.* **1999**, *72*, 179.
- (18) Zverev, V. N.; Manakov, A. I.; Khasanov, S. S.; Shibaeva, R. P.; Kusch, N. D.; Kazakova, A. V.; Buravov, L. I.; Yagubskii, E. B.; Canadell, E. *Phys. Rev.* **2006**, *B74*, 104504.
- (19) (a) Ho, A. F.; Schofield, A. J. *Phys. Rev.* **2005**, *B71*, 045101. (b) Lundin, U.; McKenzie, R. H. *Phys. Rev.* **2003**, *B68*, 081101.
- (20) (a) Jérôme, D.; Schulz, H. J. *Adv. Phys.* **2002**, *51*, 293. (b) Etemad, S. *Phys. Rev.* **1976**, *B13*, 2254.
- (21) Buravov, L. I.; Zverev, V. N.; Kazakova, A. V.; Kusch, N. D.; Manakov, A. I. *Instrum. Exp. Technol.* **2008**, *51*, 156.
- (22) Brossard, L.; Clerac, R.; Coulon, C.; Tokumoto, M.; Ziman, T.; Petrov, D. K.; Laukhin, V. N.; Naughton, M. J.; Audouard, A.; Goze, F.; Kobayashi, A.; Kobayashi, H.; Cassoux, P. *Eur. Phys. J.* **1998**, *B1*, 439.
- (23) Sato, A.; Ojima, E.; Kobayashi, H.; Hoshkoshi, Y.; Inose, K.; Kobayashi, A. *Adv. Mater.* **1999**, *11*, 1192.

JA801841Q